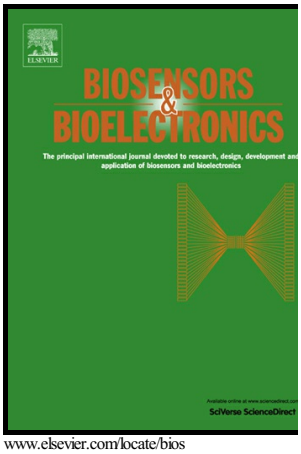

www.elsevier.com/locate/bios

$[G_3T]_5/Tb^{3+}$ based DNA biosensor with target DNA-triggered autocatalytic multi-cycle-amplification and magnetic nanoparticles assisted-background-lowered

Hong Jiang, Xiaojun Zhang, Guangfeng Wang

PII: S0956-5663(15)30301-8
DOI: http://dx.doi.org/10.1016/j.bios.2015.07.052
Reference: BIOS7870

To appear in: *Biosensors and Bioelectronic*

Received date: 19 May 2015
Revised date: 13 July 2015
Accepted date: 23 July 2015

Cite this article as: Hong Jiang, Xiaojun Zhang and Guangfeng Wang $[G_3T]_5/Tb^{3+}$ based DNA biosensor with target DNA-triggered autocatalytic multi-cycle-amplification and magnetic nanoparticles assisted-background lowered, *Biosensors and Bioelectronic* http://dx.doi.org/10.1016/j.bios.2015.07.052

$[G_3T]_5/Tb^{3+}$ based DNA biosensor with target DNA-triggered autocatalytic multi-cycle-amplification and magnetic nanoparticles assisted-background-lowered

Hong Jiang[a], Xiaojun Zhang[a], Guangfeng Wang [a,b*]

a Key Laboratory of Chem-Biosensing, Anhui province; Key Laboratory of Functional Molecular Solids, Anhui province; College of Chemistry and Materials Science, Center for Nano Science and Technology, Anhui Normal University, Wuhu 241000, PR China

b State Key Laboratory of Chemo/Biosensing and Chemometrics, Hunan University, Changsha 410082, PR China

Corresponding Author: Guangfeng Wang

E-mail: wangyuz@mail.ahnu.edu.cn

Fax: +86-553-3869303; Tel: +86-553-3869302

Abstract: Due to terbium's unique photophysical properties, nucleic-acid-sensitized terbium (DNA/Tb^{3+}) bioluminescent system becomes a potential candidate for the fabrication of DNA biosensors. However, the low sensitivity of DNA/Tb^{3+} bioluminescent system limits its development. In this paper, a strategy combining autocatalytic multi-cycle-amplification (including exonuclease III (exo III)-aided and Zn^{2+}-requiring DNAzyme-assisted target recycling amplifications) and magnetic nanoparticles assisted-background-lowering to improve the sensitivity of DNA/Tb^{3+} bioluminescent system is presented for sensitive detection of target DNA (tDNA). The DNA/Tb^{3+} bioluminescent system was investigated by ultraviolet-visible (UV-vis) absorption and luminescence spectra. The possible conjugation mechanism and mode of DNA with Tb^{3+} was discussed. The autocatalytic multi-cycle-amplification effect was investigated by the comparison of the luminescence. The carboxylation-functionalized Fe_3O_4-magnetic nanoparticles (MNPs) were characterized and its role in background lowering was proved. As a result, with the designed protocol, the detection limit for the tDNA detection reached a low level to aM, which is especially exciting for the DNA/Tb^{3+} bioluminescent system. In the process, due to the separation effect of MNPs, the assay solution was purified to avoid the nonspecific luminescence of DNA/Tb^{3+}, not only lowering the background signal greatly (about five times lower than that without the use of MNPs but also improving the reproducibility and stability. We hope that our attempt in this field will not only extend the application of DNA/Tb^{3+} luminescent system in biosensing areas but also open the road to adaptation of the protocols to other related analytes.

Keywords: nucleic-acid-sensitized terbium; DNAzyme; recycling amplifications; magnetic nanoparticles

1. Introduction

As the most important biological macromolecules in all living things, nucleic acids, including DNA and RNA, are extraordinary attractive because of their functions in encoding, transmitting and expressing genetic information (Ralph et al., 2011). So far, the development of sensors for sequence-specific and sensitive detection of DNA is being highly motivated by its various potential applications in molecular diagnostics, forensic investigations, genetics therapy and biomedical development (Wang et al., 2011; Zhou et al., 2011). In particular, the concentrations of DNA often present at a very low level in the early stage of disease. Thus, sensitive detection of DNA with extremely low amount is important (Rosi et al., 2006; Xu et al., 2009). Currently, various methods have been developed for the determination of DNA, such as luminescent (Zhou et al., 2013; Zhang et al., 2014), colorimetric (Li et al., 2012; Tang et al., 2012) and electrochemical methods (Cao et al., 2012; Nie et al., 2014). Among them, luminescent DNA detection has attracted a great deal of interest because of its high sensitivity and no requirement of complicated procedures for sample pretreatment (Yan et al., 2011). Due to its unique photophysical properties (sharply spiked emission bands, large Stokes' shifts, long lifetime and excellent biological compatibility), nucleic-acid-sensitized terbium (DNA/Tb^{3+}) bioluminescent system is hopeful to be developed for the DNA detection (Moore et al., 2009). However, to the best of our knowledge, the DNA/Tb^{3+} based DNA sensors remain much less explored except the reports of Ye B. C. et al. and Shi G. Y. et al. (Zhang and Le et al., 2013; Zhang and Qu et al., 2014). It is obvious that this lack of studies does not reflect the fact that DNA/Tb^{3+} bioluminescent composites have been ignored or that their potential has been underestimated. It is primarily due to the fact that the low sensitivity of DNA/Tb^{3+} bioluminescent system. However, sensitivity is a key factor greatly affecting the performance of the biosensor and its real application. Thus it is an urgent and challenging task to improve the sensitivity of DNA/Tb^{3+} bioluminescent system for further exploration in biosensor.

The improvement of the sensitivity is usually realized by two kinds of strategies including the amplification of the recognition events signal and the decrease of the background (Lu et al., 2011). Recently, with the development of DNA based biosensor, various DNA related signal amplification strategies have been employed to improve the sensitivity for the extreme detection capability toward target analytes, including the assembly of supersandwich structure (Wang et al., 2012), rolling circle amplification (RCA) (Zhang et al., 2015), polymerase chain reaction (PCR) (Beaudet et al., 2008; Chen et al., 2011) and so on. Owing to the simple operation and striking improvement of the high sensitivity, the development of autocatalytic cycle amplified strategy has drawn more and more concerns in DNA based biosensor (Weizmann et al., 2008), such as exonuclease III (exo III)-aided signal amplification (Wang et al., 2012) and Zn^{2+}-requiring 8-17 DNAzyme-assisted target recycling amplification (Liu et al., 2007). Because of its easy availability, high catalytic activity and wide applicability, exo III is usually used as the cleavage enzyme in the target recycling-oriented amplification. Its no requirement of any specific recognition sequence makes it an ideal candidate for the development of signal amplified detection platforms (Xuan et al., 2012; Lee et al., 2005). As for the Zn^{2+}-requiring DNAzyme, it is usually composed of a substrate strand and an enzyme strand. In the presence of Zn^{2+}, the specific cleavage of substrate strand is nicked, resulting in the substrate strand split into two fragments, one of which contains the signal molecules triggering the amplification. It also has received remarkable interests due to its merits of high sensitivity, easy operation, low cost to produce and

can be denatured and renatured many times without losing their catalytic activities toward substrates (Ali et al., 2009). Thus, it is worth expecting to combine the advantages of the exo III-with Zn^{2+}-requiring DNAzyme-assisted signal amplification to improve the sensitivity of DNA/Tb^{3+} bioluminescent system.

Besides the amplification of the signal, another way to improve the sensitivity could be carried out by lowering the background (Lu et al., 2011). Due to the rich metal-site of DNA, Tb^{3+} would easily bind to it resulting in a high background. Thus it is quite essential to solve the problem for DNA/Tb^{3+} bioluminescent system (Jung et al., 2014). Recently, the nanomaterials-based quenching method has gained the attention widely for background lowering (Zhen et al., 2010; Zhang et al., 2011). However, because signal molecules and nanoquencher usually coexist in the assay solution, there always exists the problem of quenching efficiency which may result in the limitation of lowering background. Therefore, to decrease the background thoroughly, it may be a solution to separate the signal molecules from the complex sample solutions. It then inspired us to use Fe_3O_4-magnetic nanoparticles with excellent separation capability (Willner et al., 2003; Weizmann et al., 2003) for the background lowering of DNA/Tb^{3+} bioluminescent system.

In the present work, based on the unique advantages and the urgent need of high sensitivity of DNA/Tb^{3+} bioluminescent system, a sensitive DNA/Tb^{3+} bioluminescent system with amplified signal and low background is developed for the target DNA (tDNA) detection. The exo III-aided and Zn^{2+}-requiring DNAzyme-assisted autocatalytic multi-cycle-amplification were used to amplify the signal. Meanwhile, carboxylation-functionalized Fe_3O_4-magnetic nanoparticles (MNPs) were used here to lower the background and improve the efficiency of detection through separating the signal molecules from complex sample solution and avoiding the nonspecific sensitization. Combining the strategies of lowering background with the autocatalytic multi-cycle-amplification, the ultralow detection limit down to aM level for tDNA is obtained. In addition, a satisfactory reproducibility and stability could be obtained also due to the purified assay solution separated by MNPs.

2. Experimental

All of the experimental parts were in supplemental information

3. Results and discussion

3.1. Scanning electron microscopy (SEM), fourier transform infrared spectroscopy (FTIR) and ultraviolet-visible (UV-vis) characterization.

The characterization of MNPs was implemented by means of typical SEM. As shown in Fig. 1A, the MNPs are spherical with high size uniformity and an average diameter of ~ 50 nm. To provide direct proof of the carboxyl-functionalization, FTIR spectroscopy was also investigated. As shown in Fig. 1B, the bands at 1629 and 1384 cm^{-1} are attributed to carboxyl groups. Typical bands assigning to the Fe-O stretching appear at approximately 592 cm^{-1}. It shows the MNPs were prepared successfully (Fu et al., 1999). The formation of (4)-MNPs was characterized with UV-vis absorption spectroscopy and the results were shown in Fig. 1C. No absorption peaks appear in the UV-vis spectrum of MNPs before they were conjugated with (4). After the MNPs were incubated with (4), a new absorption peak at approximately 260 nm, the UV-vis absorption maximum of

DNA, was observed in the spectrum of the mixture solution. It verified that the MNPs have been successfully functionalized with (4).

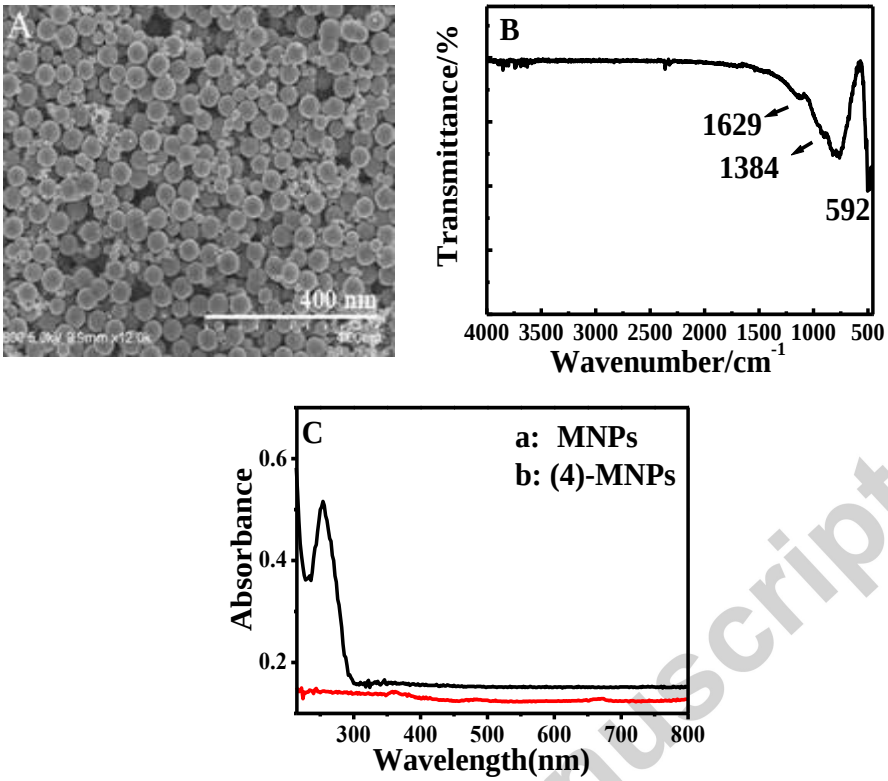

Fig.1. SEM image (A) and FTIR spectra (B) of the prepared MNPs (50 nm). (C) UV-vis absorption spectroscopy of bare MNPs (a) and (4)-MNPs (b).

3.2 The design of the sensor.

Scheme 1 schematically illustrated the proposed biosensing protocols with autocatalytic multi-cycle-amplification (Zn^{2+}-requiring DNAzyme-assisted and two-step exo III-aided autocatalytic target recycling amplifications) and MNPs-assisted-background-lowered strategy for tDNA detection. Firstly, a hairpin-like DNA probe (1) was employed in the system. The blue part of the tailored nucleic acid structure was designed containing the recognition site sequences of the tDNA. The red part corresponded to the nucleic acid sequence of 8-17 DNAzyme (Liu et al., 2007). As shown in part A of the exo III-aided autocatalytic target recycling, in the presence of the tDNA (2), its hybridization with blue part leaded the formation of a double-stranded DNA (dsDNA) with a blunt end at the 3' terminus (step a) where could be digested by exo III (step b). Then, (2) and 8-17 DNAzyme (3) can be released (step c). The liberated (2) become available to trigger the successive reaction cycle, leading to the generation of a large amount of (3). As shown in part B, the liberated (3) from the process of part A would hybridize with hairpin DNA (4)-MNPs (step d) and enter the Zn^{2+}-requiring DNAzyme-assisted target recycling amplification system. With the addition of Zn^{2+}, due to the cleavage of Zn^{2+} at the rA position of (4), the (5)-MNPs was liberated (step e) from (4). As shown in part C, the separated (5)-MNPs would be obtained by the magnetic separation in the step f and then enter the exo III'-aided autocatalytic

target recycling process. To construct DNA/Tb^{3+} bioluminescent system, (6), a hairpin-like DNA, was designed containing two parts, one was the $[G_3T]_5$ sequences and the other part was a fragment of single DNA (ssDNA) complementary with (5). Then, by the hybridization of (5)-MNPs with (6) and then the digestion of exo III' (step g), (7) were released from (6). Pure (7) solution was obtained through the second separation process (step h). Finally, as shown in part D, the Tb^{3+} solution was added to the pure solution containing (7) to monitor luminescent signal. On the basis of the above process, the signal can be exponentially amplified and meanwhile the nonspecific sensitization was avoided to lower the background. Therefore, the current biosensing protocol is hopeful to offer an ultrahigh sensitivity for the tDNA detection assay.

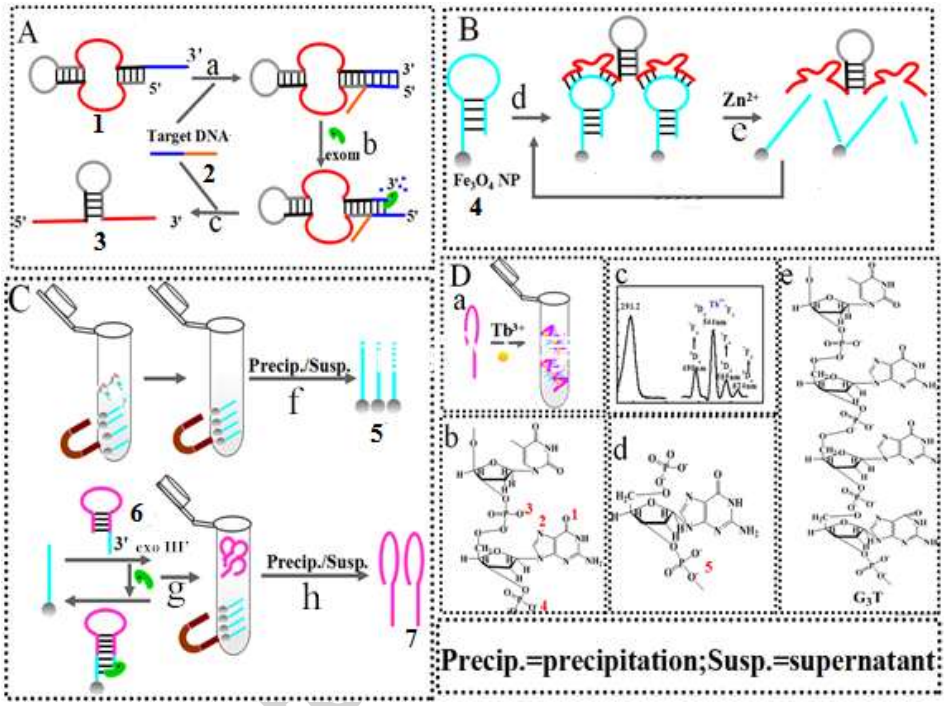

Scheme1

Scheme 1. Schematic analysis of the tDNA by the autocatalytic multi-cycle-amplification and MNPs-assisted-background-lowered strategy. (A) exo III-aided autocatalytic target recycling; (B) Zn^{2+}-requiring DNAzyme-assisted target recycling amplification system; (C) exo III'-aided autocatalytic target recycling process, (D) the scheme of the luminescent of DNA/Tb^{3+}(a), the metal binding sites of in G base (b), the luminescence of DNA/Tb^{3+}(c), one metal binding site 5 of PO_4^{3-} group in T base (d), and the possible conjugation mechanism and mode of DNA with Tb^{3+} (e).

3.3. Energy transfer (ET) and various electronic transitions in DNA/Tb^{3+} bioluminescent system.

Previous studies reveal that ssDNA can greatly enhance the Tb^{3+} emission, but dsDNA cannot (Fu et al., 1999). The specific sequence $[G_3T]_5$ was ever used to effectively sensitize and improve the luminescence of Tb^{3+}as reported (Zhang and Le et al., 2013; Zhang and Qu et al., 2014). We investigated ET of DNA/Tb^{3+} in experiment and proposed the possible mechanism. Fig. 2A is the schematic description of the luminescent character of Tb^{3+}. With the excitation of the $[G_3T]_5$ antenna, followed by intersystem crossing from its singlet state to its triplet state and subsequent ET to the terbium 5D state yields characteristic terbium phosphorescence with four sharp bands (Fig. 2A). Tb^{3+} ion with a high-energy excited state ($^5D_4$, 20500 cm^{-1}) as an energy acceptor matches the ET which lies in blue or shorter wavelength regions, resulting in the typical emission of Tb^{3+} ion arising from its $^5D_4$ excited state to $^7F_6$,$^7F_5$,$^7F_4$ and $^7F_3$ ground state with the peaks at 490, 544, 585 and 624 nm, respectively and the most intensity centralizes at 544 nm (picture c in Scheme 1D) (Fu et al., 1999). Since nucleic acids exhibit large absorption cross sections, and the triplet state of nucleic acids is slightly higher in energy than the ^5D state of the Tb^{3+}, the ET from the excited base to the emissive $^5D_4$ state of bound Tb^{3+} is possible (Formoso et al., 1973; Nagesh et al., 1992). The luminescence character of Tb^{3+} in our system was studied with luminescence and UV-vis absorption spectroscopy. As shown in Fig. 2B, Tb^{3+} solution shows a characteristic luminescence emission under excitation with 291 nm light (curve b). However, the emission is very weak maybe owing to the quenching effect of water molecules (Fu et al., 1999). In the presence of $[G_3T]_5$ (curve d), the luminescence intensity of Tb^{3+} increases significantly, due to the ET from nucleic acids to Tb^{3+} and the weak electrostatic interactions between the +3 charged terbium and the negatively charged nucleotides. Fig. 2C shows that the UV-vis absorption spectroscopy of Tb^{3+} at 203 nm greatly increases in the presence of $[G_3T]_5$. This further suggests that $[G_3T]_5$ absorbs ultraviolet radiation to sensitize the emission of Tb^{3+}. To gain more insight into the $[G_3T]_5$-sensitized luminescence of Tb^{3+}, we investigated the luminescence lifetime of Tb^{3+} in the absence and presence of $[G_3T]_5$. Fig. 2D shows that the emission lifetime of Tb^{3+} increases from 0.23 to 0.43 ms after the addition of $[G_3T]_5$. A longer emission lifetime implies the increase in the rate constant for radiative deactivation which can be ascribed to the displacement of water molecules along with a reduction in energy loss of the Tb^{3+} complexes. We suggest the results here and the reported literature are reasonable from the theory. As we know, DNA has a lot of metal binding sites, especially G-rich sequence, which can bind to Tb^{3+} slightly. In picture b of Scheme 1D, the metal binding sites of 1, 2 in G base and 3, 4 in PO_4^{3-} group can bind Tb^{3+} leading to sensitize the emission of Tb^{3+} (picture c). As shown in picture d, there is one metal binding site 5 of PO_4^{3-} group in T base. Because the lack of one site of three G (G_3) bases can't bind Tb stably and meanwhile T base can provide one site from PO_4^{3-} group, in order to fully sensitize the emission of Tb^{3+}, $[G_3T]$ unit may be the optimum sequence. Due to the binding effect, when G-rich DNA binds to Tb^{3+}, the construction of the DNA is suggested as the picture e in Scheme 1D.

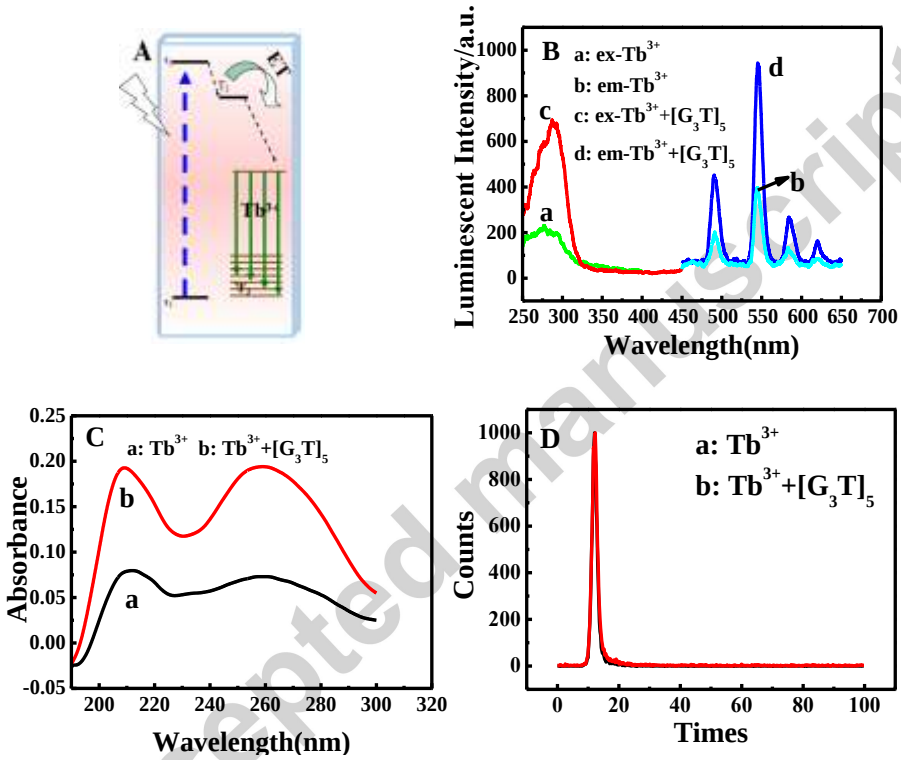

Fig. 2. (A) Illustration of ET in conjunction with various electronic transitions between DNA and Tb^{3+} ions. (B) Excitation spectrum (λ^{ex}=290 nm) (a, c) and emission spectrum (λ^{em}= 490, 544, 585 and 624 nm) (b, d) of 2 μM Tb^{3+} solution in the absence (a, b) and presence (c, d) of 3 μM $[G_3T]_5$. (C) UV-vis absorption spectroscopy of Tb^{3+} solution in the absence (a) and presence (b) of $[G_3T]_5$. (D) Luminescence lifetime of Tb^{3+} in the absence (a) and presence (b) of $[G_3T]_5$ in aqueous solution.

3.4. The feasibility of the DNA/Tb^{3+} bioluminescent system toward the detection of tDNA.

In order to investigate the feasibility of the biosensor, the luminescence in the stepwise procedure is shown in Fig. 3A. As shown in curve a of Fig. 3A, in the absence of tDNA, there only exists a slight background luminescence. We suggest the reason may be that without tDNA, $[G_3T]_5$ could not be liberated from (6) in step g and finally the extracted (6) with hairpin structure can't sensitize the fluorescence of Tb^{3+}. However, the existence of a bit of ssDNA in 3' end of (6) can sensitize the luminescence of Tb^{3+} slightly. Curve e in Fig. 3A shows that an obvious enhancement is observed in the presence of tDNA, suggesting that tDNA triggers the successive process as we designed. To confirm the effect of exo III in the proposed autocatalytic multi-cycle-amplification system, the control experiment is carried out with tDNA in the absence and presence of exo III. As shown in curve b and e of Fig. 3A, we can see that the presence of exo III (curve e) causes an increase in luminescence intensity compared with that without exo III (curve b). Such increase is basically due to that the exo III, which can bind to the duplex region and catalyze the stepwise removal of mononucleotides, liberate (2) and (3) to trigger the signal amplification. Furthermore, the role of Zn^{2+} is also studied in the proposed system. Compared curve c with e in Fig. 3A, the luminescent intensity of curve e in the presence of Zn^{2+} is stronger than that of curve c without Zn^{2+}. The results can illustrate that Zn^{2+} plays an important role in signal amplification as designed. At last, we also investigate the effect of exo III', as shown in curve d and e of Fig. 3A, the luminescent value of curve e in the presence of exo III' is much higher than that of curve d without the addition of exo III', verifying the importance and necessity of exo III' in the biosensing protocols. Fig. 3A, inset, shows the obvious difference of the luminescence intensity clearly under the condition of the corresponding curve (a), (b), (c) and (d). We use agarose gel electrophoresis to confirm the formation of the final products in part A, part B and part C. As shown in Fig. 3C, there are bright bands in lane a which is the final products in part A. The final products in part B (lane b) is similar to lane a and the final products in part C (line c) moves significantly slower than lane a and b, which can verify the feasibility of the cycle process.

In order to verify the outstanding feature of the background lowering by employing MNPs in the proposed biosensor, (4) without the modification of MNP, is designed for comparison. Fig. 3B shows the background luminescence intensities of $[G_3T]_5/Tb^{3+}$ with modified and unmodified MNPs. The background luminescence intensities of $[G_3T]_5/Tb^{3+}$ is ultralow with the assisted MNPs which has an excellent separation ability (curve a). The luminescence value is 68.7 (curve a in Fig. 3B), about five times lower than that without the assist of MNPs (L=318, curve b in Fig. 3B). We can summary that the proposed biosensor with MNPs shows a relatively low background because of the use of MNPs.

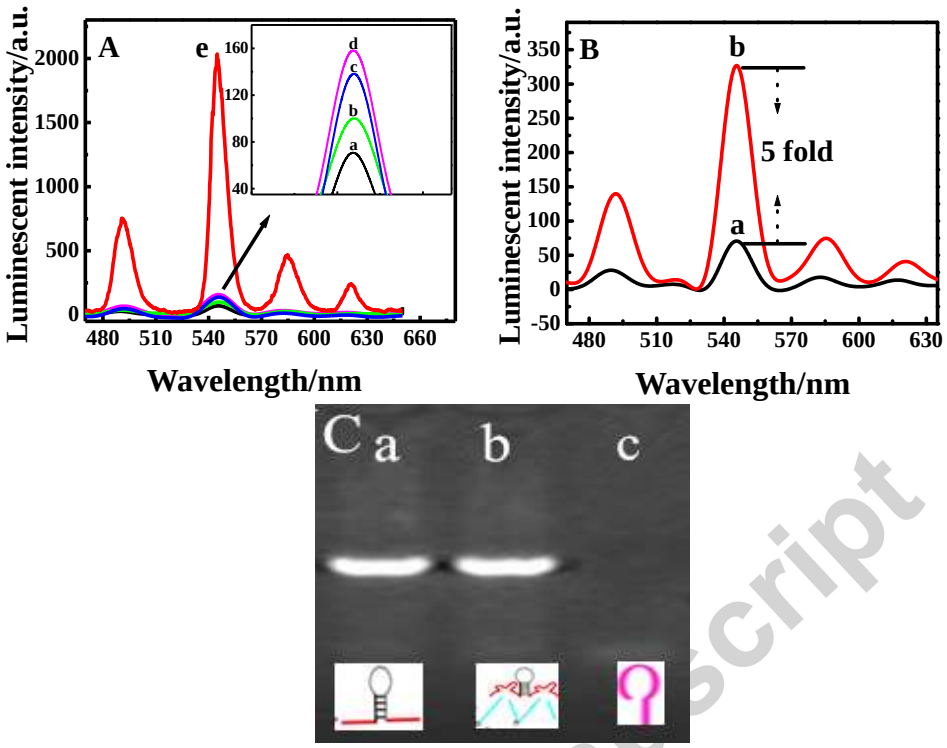

Fig. 3. (A) Luminescence response of the solution containing (a) (1)+exo III+Zn^{2+}+exo III', (b) (1)+tDNA+Zn^{2+}+exo III', (c) (1)+tDNA+exo III+exo III', (d) (1)+tDNA+exo III+Zn^{2+} and (e) (1)+tDNA+exo III+Zn^{2+}+exo III'; The inset shows the luminescence intensity in the condition of (a), (b), (c) and (d). (B) Luminescence response of the biosensing protocols modified with (a) and without (b) MNPs. (C) Agarose gel electrophoresis image for autocatalytic multi-cycle-amplification assay: the final products in part A (lane a), B(lane b) and C(lane c). The inset is the schematic illustration of the final products in part A, B and C, respectively.

3.5. Optimization of assay conditions.

The detection sensitivity of the proposed biosensing protocols was influenced by the experimental condition. In the exo III-aided autocatalytic target recycling system, the concentration and digestion time of exo III were investigated. Fig. 4A shows that the value of L/L_0 increases with the concentration of exo III until the concentrations is 10 U (Fig. 4A) and the value of L/L_0 increases with the digestion time and the maximum value of L/L_0 is obtained when the digestion time of exo III is 30 min (Fig. 4B). To achieve the best performance for Zn^{2+}-requiring DNAzyme-assisted target recycling amplification, the concentration of cofactor Zn^{2+} and the catalytic time of the DNAzyme were also optimized, respectively. The maximum value of L/L_0 is obtained when the Zn^{2+} concentration is 1.0 nM (Fig. 4C) and the catalytic time of DNAzyme is 40 min (Fig. 4D). At last, the concentration of exo III' and Tb^{3+} was investigated in the exo III'-aided autocatalytic target recycling system. The optimized concentration of exo III' is 12 U (Fig. 4E) and Tb^{3+} is 0.2 nM (Fig. 4F).

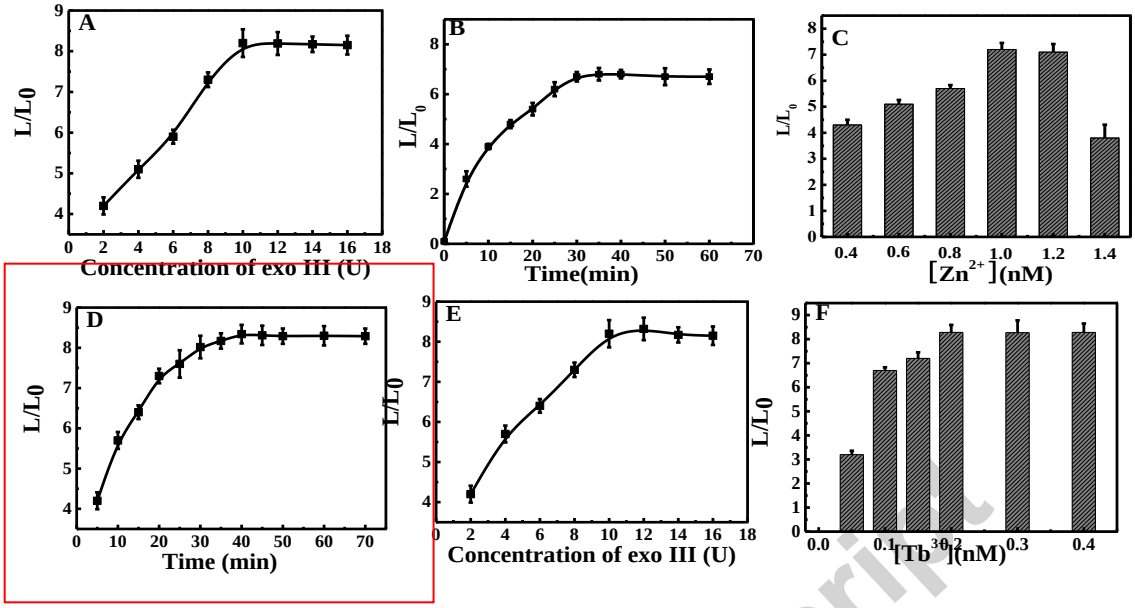

Fig. 4. Variance of the value of L/L_0 with exo III concentration from 2 to 16 U (A) and digestion reaction time from 0 to 60 min (B) in the exo III-aided autocatalytic target recycling system. Variance of the value of L/L_0 with the concentration of Zn^{2+} (0.4, 0.6, 0.8, 1.0, 1.2 and 1.4 nM) (C) and the catalytic time from 0 to 70 min (D) in the Zn^{2+}-requiring DNAzyme-assisted target recycling amplification system. Variance of the value of L/L_0 with the concentration of exo III' from 2 to 16 U (E) and the concentration of Tb^{3+} (0.05, 0.1, 0.15, 0.2, 0.3 and 0.4 nM); (F) in the exo III'-aided autocatalytic target recycling system. L and L_0 are the luminescent intensity of the sensing system in the presence and absence of tDNA. Error bars show the standard deviations of measurements taken from three independent experiments.

3.6. Detection of tDNA.

The calibration curve for tDNA by this sensing system is shown in Fig. 5. Under the optimal experimental conditions, with the increasing concentrations of tDNA to the sensing system, the gradual luminescence increases as depicted in Fig. 5A. Fig. 5B shows that the luminescent intensity exhibits a linear correlation with the logarithmic of tDNA concentration from 0 to 0.1 nM. The correlation equation is $L=209.7\log_{10}{}^{[tDNA]}+4043$ ($R^2= 0.9920$) and the detection limit of tDNA (3δ/slope) is approximately 0.5 aM. Thus, the detection limit is much lower than that of the previously reported $[G_3T]_5/Tb^{3+}$ bioluminescence system for tDNA (0.05 μM) (Tang et al., 2012). Furthermore, the detection limit is lower than the reported cycle amplified assay (Table S2).

To prove the signal amplification effect by the proposed biosensing protocols, another one-step amplification procedure was also designed for comparison. In this sensing system, a simple hairpin (6) was designed as a probe. In the presence of tDNA, (6) recognize the tDNA and form the dsDNA which contain a blunt end at the 3' terminus. The dsDNA can be digested with the addition of exo III, which can trigger the release of the tDNA and $[G_3T]_5$, and then $[G_3T]_5$ can sensitize the luminescence of Tb^{3+} (Fig. 5C). Fig. 5D depicts that the luminescence intensity

increases with the increasing concentration of tDNA from 0 to 300 nM. Fig. 5E shows the derived calibration curve indicating that tDNA can be analyzed by the $[G_3T]_5/Tb^{3+}$ based one-step amplification biosensor with a detection limit corresponding to 30 nM (3δ/slope) and a calibration function of L=2.463[tDNA]+428.4 (R^2= 0.9934). However, the high background signal and low sensitivity proved to be a disappointment. Based on these results, the sensitivity based on our autocatalytic multi-cycle-amplification and background lowering is superior to the one-cycle-amplification.

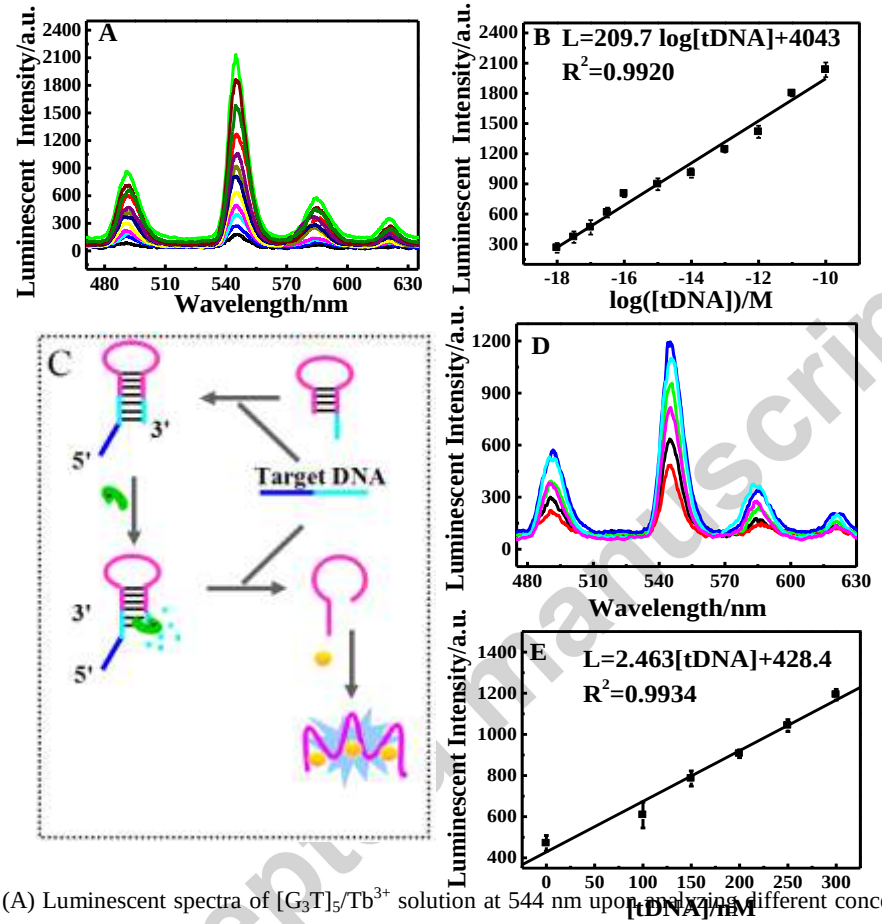

Fig. 5. (A) Luminescent spectra of $[G_3T]_5/Tb^{3+}$ solution at 544 nm upon analyzing different concentrations of the tDNA from 0 to 1 μM (from bottom to top) by the autocatalytic multi-cycle-amplification and MNPs-assisted-background-lowered strategy. (B) Relationship between the luminescent intensity at 544 nm and the logarithmic concentrations of tDNA by the autocatalytic multi-cycle-amplification and MNPs-assisted-background-lowered strategy. (C) Schematic analysis of the tDNA by the one-step amplification system; (D) Luminescent spectra of $[G_3T]_5/Tb^{3+}$ solution upon analyzing different concentrations of the tDNA from 0 to 300 nM (from bottom to top) in the one-step amplification system; (E) Relationship between the luminescent intensity at 544 nm and the concentrations of tDNA in one-step amplified system. Error bars represent standard deviations of measurements (n=3).

3.7. Specificity, practicality，reproducibility and stability of the $[G_3T]_5/Tb^{3+}$ biosensor.

The sequence discrimination of the autocatalytic multi-cycle-amplification and background-lowered $[G_3T]_5/Tb^{3+}$ system was investigated (Fig. S1). The specific response of the biosensing system to tDNA is evaluated by examining the luminescence signal of the $[G_3T]_5/Tb^{3+}$ solution in the presence of various DNA (single-base-mismatched (8), two-base-mismatched (9), three-base-mismatched oligonucleotides (10)) under the same conditions. The result shows that only the addition of tDNA can induce a prominent increase in the luminescence emission of the $[G_3T]_5/Tb^{3+}$ biosensor, whereas the addition of other mismatched DNA causes only very slight luminescence changes, demonstrating that our sensing system has a high specificity for tDNA. In addition, the practicality of the proposed strategy was also investigated by detecting tDNA by analyzing different dilution ratios (1:50, 1:100) of human serum samples under the same detection procedure as that described in the aforementioned experiment. The experimental results in Table S3 confirm the effectiveness of this proposed strategy for the determination of tDNA in human serum samples, suggesting a good practicality.

As for biosensors, not only the sensitivity and specificity but other two factors (reproducibility and stability) should also be taken into account. Surprisingly, it is found that the use of MNPs can improve the reproducibility and stability obviously besides its role of lowering the background. The reproducibility and stability of the above proposed biosensing protocol was investigated with or without the use of MNPs. Fig. S2A and Fig. S2B shows the relative standard derivation of eleven independent tests for 10 nM tDNA with the (4)-MNPs (Fig. S2A) and (4) (Fig. S2B) is 3.0% and 8.5%, respectively. It verifies that the good reproducibility in the biosensing protocol is kept with (4)-MNPs. Furthermore, Fig. S2C and Fig. S2D shows the stability of the proposed biosensing protocols with (4)-MNPs (Fig. S2C) and (4) (Fig. S2D). Fig. S2C shows the luminescence response of the $[G_3T]_5/Tb^{3+}$ biosensor in the autocatalytic multi-cycle-amplification strategy to tDNA (10 nM) has no apparent change in the continuous seven days by everyday use and Fig. S2D shows apparent change, verifying the good stability with (4)-MNPs. The satisfactory stability and reproducibility is ascribed to the probably reason. The most traditional separation effect of MNPs results in a purified solution allowing the luminescence sensitization of $[G_3T]_5/Tb^{3+}$, avoiding the nonspecific luminescence and then improving the reproducibility and stability.

4. Conclusions

In conclusion, we have designed a sensitive $[G_3T]_5/Tb^{3+}$ based luminescent assay for the detection of tDNA with autocatalytic multi-cycle-amplification and MNPs-assisted-background-lowered strategy. In this system, autocatalytic multi-cycle-amplification including autocatalytic exo III-aided and Zn^{2+}-requiring DNAzyme-assisted target recycling amplification, is applied to improve the sensitivity of DNA/Tb^{3+} bioluminescent system. Furthermore, we find that the MNPs play an important role in two sides. The separation effect of MNPs allows it to sensitize the luminescence of $[G_3T]_5/Tb^{3+}$ in the purified solution avoiding the nonspecific luminescence of $[G_3T]_5/Tb^{3+}$, which not only decreased the background signal, about five times lower than that without the use of MNPs, but also improved the reproducibility and stability. As a result, the biosensing protocol reached a satisfactory sensitivity, reproducibility and stability. To the best of our knowledge, there was little research that focuses on the autocatalytic signal amplification esp. adapting a Zn^{2+}-requiring DNAzyme and exo III-aided target cycle amplification in DNA/Tb^{3+} bioluminescent system for tDNA detection**.** Our attempt in this field will not only extend the application of DNA/Tb^{3+} bioluminescent system in biosensing areas but also open the road to adaptation of the protocols to other related analytes.

Acknowledgements

This work is financially supported by the Projects (21073001, 21005001 and 21371007) from National Natural Science Foundation of China, Natural Science Foundation of Anhui (KJ2009B013Z) the project of Anhui Key Laboratory of Controllable Chemistry Reaction & Material Chemical Engineering (OFCC0905), and the Young Teacher Program of Anhui Normal University (2009xqnzc19).

References

Ali, M. M., Li, Y., 2009. Angew. Chem. Int. Ed. 48, 3512-3515.

Beaudet, A. L., Belmont, J. W., 2008. Annu. Rev. Med. 59, 113-129.

Cao, Y., Zhu, S., Yu, J. C., Zhu, X. J., Yin, Y. M., Li, G. X., 2012. Anal. Chem. 84, 4314.

Chen, P., Pan, D., Fan, C. H., Chen, J. H., Huang, K., Wang, D. F., Zhang, H. L., Li, Y., Feng, G. Y., Liang, P. J., He, L., Shi, Y. Y., 2011. Nat. Nanotechnol. 6, 639-644.

Formoso, C., Biochem., Biophys., 1973. Res. Commun. 53, 1084.

Fu, P. K. L., Turro, C., 1999. J. Am. Chem. Soc. 121, 1-2.

Jung, P., Huang, J., Liu. J.W., 2014. Anal. Chem. 86, 5999-6005.

Lee, H. J., Li, Y., Wark, A. W., Corn, R. M., 2005. Anal. Chem. 77, 5096-5100.

Li, J., Fu, H. E., Wu, L. J., Zheng, A. X., Chen, G. N., Yang, H. H., 2012. Anal. Chem. 84, 5309.

Liu, J., Lu, Y., 2007. Angew. Chem. Int. Ed. 46, 7587-7590.

Lu, L. M., Zhang, X. B., Kong, R. M., Yang, B., Tan, W. H., 2011. J. Am. Chem. Soc. 133, 11686-11691.

Moore, E. G., Samuel, A. P., Raymond, K. N., 2009. Acc. Chem. Res. 42, 542.

Nagesh, N., Bhargava, P., Chatterji, D., 1992. Biopolymers. 32, 1421.

Nie, J., Zhang, D. W., Zhang, F. T., Yuan, F., Zhou, Y. L., Zhang, X. X., 2014. Chem. Commun. 50, 6211.

Ralph, E. K., Christoph, E., Dumelinz., David, R. L., 2011. Chem. Soc. Rev. 40, 5707-5717.

Rosi, N. L., Giljohann, D. A., Thaxton, C. S., Lytton-Jean, A. K. R., Han, M. S., Mirkin, C. A., 2006. Science. 312, 1027.

Tang, L. H., Liu,Y., Ali, M. M., Kang, D. K., Zhao, W. A., Li, J. H., 2012. Anal. Chem. 84, 4711.

Wang, F., Elbaz, J., Orbach, R., Magen, N., Willner, I., 2011. J. Am. Chem. Soc. 133, 17149.

Wang, F., Elbaz, J., Willner, I., 2012. J. Am. Chem. Soc. 134, 5504-5507.

Wang, G. F., Huang, H., Wang, B. J., Zhang, X. J., Wang, L., 2012. Chem. Commun. 48, 720-722.

Weizmann, Y., Cheglakov, Z., Willner, I., 2008. J. Am. Chem. Soc. 130, 17224-17225.

Weizmann, Y., Patolsky, F., Katz, E., Willner, I., 2003. J. Am. Chem. Soc. 125, 3452-3454.

Willner, I., Katz, E., 2003. Angew. Chem., Int. Ed. 42, 4576-4588.

Xu, W., Xue, X., Li, T., Zeng, H., Liu, X., 2009. Angew. Chem., Int. Ed. 48, 6849.

Xuan, F., Luo, X., Hsing, I. M., 2012. Anal. Chem. 84, 5216-5220.

Yan. H., Wang. H. F., 2011. Anal. Chem. 83, 8589-8595.

Zhang, M., Le, H. N., Jiang, X. Q., Yin, B. C., Ye, B. C., 2013. Anal. Chem. 85, 11665-11674.

Zhang, M., Qu, Z. B., Ma, H. Y., Zhou, T. S., Shi, G. Y., 2014. Chem. Commun. 50, 4677-4679.

Zhang, P., Wu, X. Y.,Yuan, R., Chai, Y. Q., 2015. Anal. Chem. 87, 3202-3207.

Zhang, Y., Wang, L. J., Zhang, C. C., 2014. Chem. Commun. 50, 1909.

Zhang, Y., Liu, Y., Zhen, S. J., Huang, C. Z., 2011. Chem. Commun. 47, 11718-11720.

Zhen, S. J., Chen, L. Q., Xiao, S. J., Li, Y. F., Hu, P. P., Zhan, L., Peng, L., Song, E. Q., Huang, C. Z., 2010. Anal. Chem. 82, 8432-8437.

Zhou, H., Xie, S. J., Zhang, S. B., Shen, G. L., Yu, R. Q., Wu, Z. S., 2013. Chem. Commun. 49, 2448.

Zhou, M., Dong, S. J., 2011. Acc. Chem. Res. 44, 1232.

Highlight

1. The sensitivity of DNA/Tb^{3+} luminescent system was improved greatly.

2. Exo III and Zn^{2+} assisted autocatalytic multi-cyclic amplification was combined.

3. Magnetic nanoparticles assisted background lowering was applied.

4. The separation effect of MNPs also brought an improved regenerability and stability.

5. The possible conjugated mechanism of [G_3T] with Tb^{3+} was discussed.